EXPERIMENTAL MEASUREMENTS ON TEMPERATURE GRADIENTS IN CONCRETE BOX-GIRDER BRIDGE UNDER ENVIRONMENTAL LOADINGS

S. R. Abid[1], N. Tayşi[2], M. Özakça[3]

ABSTRACT

The effect of the fluctuation of air temperature and solar radiation had been recognized as one of the issues that should be considered in bridge design. The effect of the daily temperature rise and drop can leads to serious thermal movements or stresses along the span of the bridge. Moreover, the nonlinear temperature gradients along the depth of the bridge superstructure, if not considered in design, can result in additional induced stresses. During the early age of concrete bridges, the hydration heat of concrete is added to the daily environmental thermal loads.

In this paper, results from experimental research on temperature gradients during the early age of a concrete bridge segment are discussed. In the current experimental study, a full-scale concrete box-girder bridge segment was instrumented with 48 type-T thermocouples to monitor the early age temperature distributions in concrete bridges. In addition, the ambient air temperature, the solar radiation and the wind speed were continuously recorded using air temperature probe, pyranometer and anemometer, respectively, which were all installed on the experimental bridge segment.

The results showed that concrete temperatures at early ages are influenced by the environmental thermal loads and the hydration heat of concrete. The degree of influence of each of which depends mainly on the location of thermocouples. The maximum vertical temperature gradient was approximately 25 ℃, which was recorded after about 12 hours from the cast of the bridge segment.

[1]Graduate Student Researcher, Dept. of Civil Engineering, University of Gaziantep, Gaziantep, Turkey, 27310

[2]Professor Asst., Dept. of Civil Engineering, University of Gaziantep, Gaziantep, Turkey, 27310

[3]Professor, Dept. of Civil Engineering, University of Gaziantep, Gaziantep, Turkey, 27310

EXPERIMENTAL MEASUREMENTS ON TEMPERATURE GRADIENTS IN CONCRETE BOX-GIRDER BRIDGE UNDER ENVIRONMENTAL LOADINGS

S. R. Abid[1], N. Tayşi[2], M. Özakça[3]

ABSTRACT

The effect of the fluctuation of air temperature and solar radiation had been recognized as one of the issues that should be considered in bridge design. The effect of the daily temperature rise and drop can leads to serious thermal movements or stresses along the span of the bridge. Moreover, the nonlinear temperature gradients along the depth of the bridge superstructure, if not considered in design, can result in additional induced stresses. During the early age of concrete bridges, the hydration heat of concrete is added to the daily environmental thermal loads.

In this paper, results from experimental research on temperature gradients during the early age of a concrete bridge segment are discussed. In the current experimental study, a full-scale concrete box-girder bridge segment was instrumented with 48 type-T thermocouples to monitor the early age temperature distributions in concrete bridges. In addition, the ambient air temperature, the solar radiation and the wind speed were continuously recorded using air temperature probe, pyranometer and anemometer, respectively, which were all installed on the experimental bridge segment.

The results showed that concrete temperatures at early ages are influenced by the environmental thermal loads and the hydration heat of concrete. The degree of influence of each of which depends mainly on the location of thermocouples. The maximum vertical temperature gradient was approximately 25 ℃, which was recorded after about 12 hours from the cast of the bridge segment.

Keywords: *Concrete bridge, box-girder, temperature gradient, solar radiation, early age, air temperature*

Introduction

Thermal effects are among many factors that have their impact on both fresh and hardened concrete. Internal and external thermal loads during the early and the late ages of concrete bridges and concrete bridge decks cause additional deformations and stresses that lead to concrete cracking [1-6]. During early ages, the heat produced in concrete due to cement hydration is an additional thermal load that is added to the daily-fluctuated air temperature and solar radiation. The superposition of hydration heat and environmental thermal loads is considered as one of the causes of early age cracks of bridge members [7-9].

[1]Graduate Student Researcher, Dept. of Civil Engineering, University of Gaziantep, Gaziantep, Turkey, 27310

[2]Professor Asst., Dept. of Civil Engineering, University of Gaziantep, Gaziantep, Turkey, 27310

[3]Professor, Dept. of Civil Engineering, University of Gaziantep, Gaziantep, Turkey, 27310

The total amount of heat released due to cement hydration reaches up to 500 joules per gram for ordinary portland cement [10]. The dissipation of heat from concrete interiors depends on the degree of sealant from formwork, the area of surfaces exposed to the ambient air, the temperature of air and the speed of wind on exposed surfaces. The dissipation of hydration heat from the cores of concrete sections to their surfaces and hence to the surroundings takes place slowly because of the low conductivity of concrete. The concrete conductivity ranges from 1.5 to 2.5 W/mK [11]. Thus, the hydration heat is generated in faster rate than its dissipation and hence leads to heat concentration in the cores of concrete sections [10].

The daily changes of solar radiation and air temperature cause vertical nonlinear temperature gradients along the depth of the bridge superstructure, which lead to induced stresses that may cause rotational distortions of the superstructure [2]. Because of its importance, the vertical nonlinear temperature gradients are considered in most of the current bridge design codes such as BS5400 [12], AASHTO LRFD [13], AS 5100 [14] and others.

The aim of this paper is to focus on temperature gradients that occur during the early age of concrete box-girder bridges due to the combined effect of hydration heat and environmental loads. For this purpose, a cast in place box-girder segment with full scale, which was instrumented with thermocouples and environmental sensors, was constructed to monitor the time-dependent temperature variations in concrete bridges during the early ages.

The Experimental Box-Girder Segment and the Instrumentation

A full-scale concrete bridge box-girder segment was constructed in the campus of Gaziantep University to study the temperature distributions and gradients in concrete bridges under environmental conditions. Fig. 1 shows the dimensions of the cross-section of the experimental box-girder segment. The average 28 days cube strength of the used concrete was 35 MPa. The concrete of the box-girder segment was cast on May 25 using two truck mixers. The bottom slab was cast first using the first truck mixer, while after 50 minutes the casting of webs and top slab was carried out using the second truck mixer. Fig. 2 shows the casting of the concrete box-girder segment.

To monitor the temperature of concrete, 48 thermocouples were used. The thermocouples were Type-T and were divided into four groups, which are the south web (S), the north web (N), the top slab (T), and the bottom slab (B) groups. The S group, the N group and the T group are consist of 13 thermocouples each, which are termed as S1 to S13, N1 to N13 and T1 to T13, respectively. However, the bottom slab group consists of 9 thermocouples only, B1 to B9. Fig. 1 illustrates the locations of the 48 thermocouples.

In addition to thermocouples, air temperature probe with solar shield, pyranometer and anemometer were installed to record the air temperature, the solar radiation and the wind speed, respectively. All thermocouples and environmental sensors were connected to data logger and data multiplexers that are continuously read and record all measurements at time steps of 30 minutes.

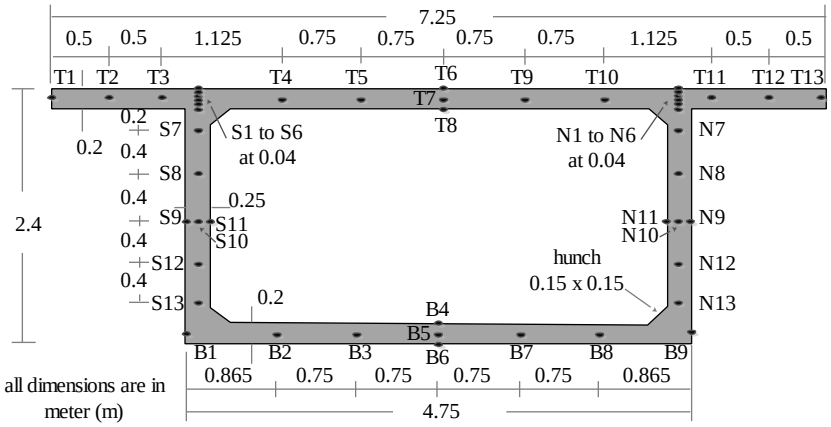

Figure 1 Dimensions of the cross-section of the box-girder segment and the locations of thermocouple

Figure 2 Concrete casting of the experimental full-scale box-girder segment

Air Temperature, Solar Radiation and Wind Speed

Fig. 3 shows the air temperature measurements and the measurements of the global solar radiation for the first five days (120 hours) after the concrete casting of the bridge segment. During the first 120 hours, the temperature of the ambient air was in the range of 10.6℃ to 30℃. The sky was partially cloudy during the first two days, the fourth day and the fifth day. The fluctuation of solar radiation intensity is clear in Fig. 3 for these days and especially for the day of concrete casting. The maximum recoded hourly solar radiation during the five days was 1040 W/m^2, which was recorded during the fourth day. The wind speed during the five days ranged from 0 m/s to approximately 3.0 m/s.

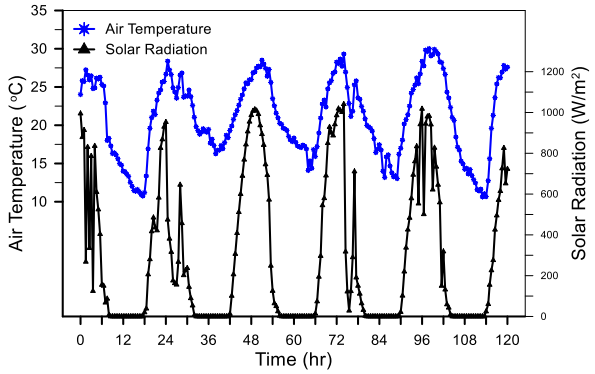

Figure 3 Air temperature and solar radiation records during the first 120 hours

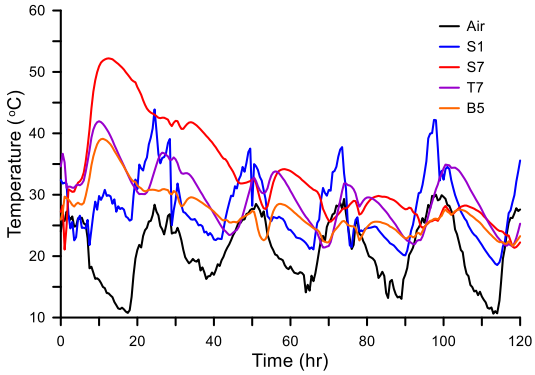

Figure 4 Temperature time curves during the 120 hours for Air, S1, S7, T7, and B5

Temperature-Time Curves

Fig. 4 shows the temperature-time curves for selected thermocouples. The selected thermocouples are S1, S7, T7 and B5. The temperature distributions along the south web and north web were found to be almost the same, therefore S1 and S7 can be considered as representative thermocouples for all the thermocouples that installed in the webs. S1 is located at the top surface of the girder (along the south web), while S7 is located 0.4 m below the top surface, and is surrounded by the largest amount of concrete as shown in Fig. 1. It is clear from the observation of Fig. 4 that among all other thermocouples, the highest effect of hydration heat was recorded at S7. The temperature increased significantly during the first 12 hours after concrete casting in spite of the low temperatures of air along these night hours, reaching a peak temperature of 52.2℃ at 11:30 p.m. (10 hours after the completion of concrete casting). Along the next 36 hours, the temperature of S7 decreased continuously showing a semi stabilization period during the mid hours of the next day. After about 2 days from concrete casting, the effect of hydration heat became limited. On the other hand, S1, which is a surface thermocouple showed much lower degree of fellowship to the hydration heat behavior even during the early hours, during which the effect of hydration heat was maximum. S1 showed stronger dependency on the fluctuation of air temperature as clearly shown in Fig. 4.

Thermocouples T7 and B5 were installed at the centeroids of the top and the bottom slabs, in which one surface is exposed to air, while the second is sealed with the formwork. Both T7 and B5 showed a mode of mixed dependency on both hydration heat and air temperature. During the early hours, the temperature of T7 and B5 increased due to the released heat from cement hydration, but the maximum temperature reached at the peak time around the mid of the first night was obviously lower than of that of S7. This can be attributed to air convection on the exposed surfaces, which decreased the surface temperate significantly, but its effect on T7 and B5 was lower because of the low concrete conductivity. During the next day, T7 showed closer behavior to that of air temperature, while B5 showed closer behavior to S1. This is mainly due to the retarded speed of air on the top surface of the bottom slab, hence the lower degree of convection compared to that of the top slab and to the shading effect on the top surface of the bottom slab by webs during the hot hours of the day.

Temperature Gradients-Time Curves

The temperature gradients along the south web were calculated based on the supposed hottest and coldest points, these were S1 and S7, considering positive gradients occurs when the top surface is hotter than interiors, the gradients were calculated by subtracting S7 from S1. The same stands for north web, the gradients were calculated by subtracting N7 from N1. Similarly, the gradients across the thicknesses of the top slab and the bottom slab were calculated based on T6, T8 and B4, B6, respectively. Fig. 5 shows the calculated gradients during the early 120 hours.

The figure clearly illustrates the effect of hydration heat on the behavior of temperature gradients. In aged concrete, top surfaces worm during the day sunny hours causing positive gradients along webs, while during the night cooling hours, top surfaces loose temperature by convection leading to negative gradients.

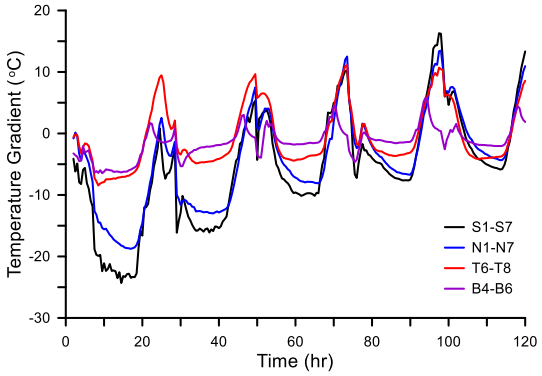

Figure 5 Temperature gradient-time curves for south web (S1-S7), north web (N1-N7), top slab (T6-T8) and bottom slab (B4-B6)

The observed behavior of north web and south web during the early hours was different. The hot interiors due to hydration heat caused negative gradients along the day and the night hours of the first day. During the following day hours, the surface wormed gradually, while the temperature of interiors kept dropping due to the decreasing effect of hydration heat. Although, the gradients of the south web during the full day hours of the next day were negative except at midday (12:00 p.m.), at which a positive gradient of 0.85℃ occurred.

The day hours of the third day, which was sunny, showed the real decrease of the effect of hydration heat. The gradient along the south web as shown in Fig. 5 was positive from 10:00 a.m. to 5:30 p.m., with a maximum positive gradient of 5.3℃ at 1:00 p.m. During the following days, the effect of hydration heat was diminishing gradually, so that gradient-time behavior became normal with positive gradients during the day hours and negative during the night hours. As shown in Fig. 5, the gradient of the north web exhibited exactly the same behavior of that of the south web.

The gradient-time curves of the top slab showed different behavior from those of webs. First, the gradient was also negative during the full day and night hours of the first day, but with much lower negative values. The maximum negative gradient during the first night was 24.3℃ for the south web, while it was only 8.5℃ for top slab. Second, during the day hours of the second day,

the positive gradient region was wider and with higher altitude than for webs. The gradient became positive from 8:30 a.m. to 4:00 p.m. with a maximum positive gradient of 9.5℃.
The behavior of the gradient of the bottom was close to that of top slab during the first day, but with lower values of both positive and negative gradients. This is mainly because the degree of exposure to solar radiation during the day hours (worming) and to fluent air during night hours (convection cooling) was obviously lower than for top slab. On the other hand, the behavior of bottom slab's gradient was closer to that of webs at some time intervals, especially during the day hours of the second and third days. The configuration of the box girder, allowed to solar heating of the bottom slab during the early morning hours and the late afternoon hours only, while during midday hours, webs mostly shaded the top surface of the bottom slab. Thus, during day hours, the gradient behavior of the bottom slab differed from those of top slab and webs.

Vertical Temperature Distributions

The understanding of the temperature distributions along the depth of bridge superstructures is important to limit the stresses that may arise from temperature gradients between the top and the bottom surfaces of the superstructure.
During the day hours, the top surface of the superstructure is directly exposed to solar radiation and hence absorbs higher thermal radiation than other parts of the superstructure, which leads to higher heat gain, hence increase the temperature of the top surface. Within the hot day hours, the top surface reaches its maximum temperature, while at the same time the concrete cores still cold, which leads to high temperature difference along the depth, which is also termed as temperature gradient.
During night hours, the opposite stands. The quick cooling of the top surface leads to a quick decrease in the temperature of the surface. Due to the low thermal conductivity of concrete, the concrete cores loose heat slowly, which causes a negative thermal gradient, with minimum temperature at the top surface and maximum at concrete cores.
Fig. 6 shows three temperature distributions during the first 25 hours, which are the temperature distribution at 2:00 p.m. (after about 1 hour after the completion of concrete pouring), the temperature distribution after about 12 hours (next morning at 2:00 a.m.) and the temperature distribution at 2:00 p.m. in the next day (after about 24 hours). From the observation of Fig. 6(a), it is clear that temperature was almost uniform along the depth of the south web at 2:00 p.m. of the first day. This observation is more obvious in Fig. 6(b) for the north web. This is because concrete was just poured 1 hour age, and hence the initial temperature of concrete controlled at this time.
After 12 hours (at 2:00 a.m.), it is obvious how the hydration heat affected the concrete temperature. The concrete temperature increased from an average of approximately 30℃ to approximately 50℃. The figure also confirms the conclusion of the previous sections, in which temperature was found to be maximum at S7 that was about 52℃. On the other hand, the cooling air was effective on the temperature of the top surface and the within top slab thermocouples as shown in Figs. 6(a) and 6(b). The temperature at the top surface was minimum at this time due to the convection cooling, which was about 27℃. Heat loss decreased as the depth of the thermocouple inside concrete increased.
To understand the limits of the effect of hydration heat on vertical temperature distributions, the vertical temperature distributions were studied for five days from concrete pouring. Fig. 7 compares the temperature distributions at 1:00 p.m. for the first five days.

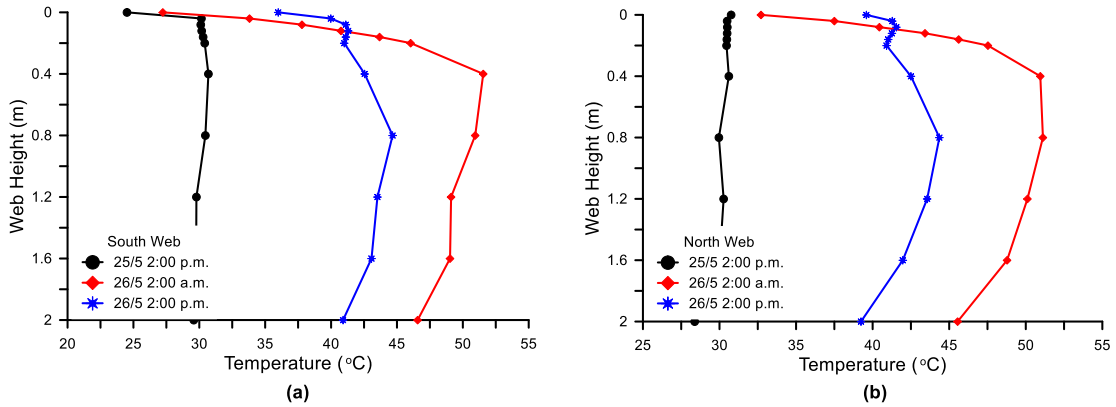

Figure 6 Vertical temperature distributions for selected time steps (a) south web (b) north web

As shown in Figs. 7(a) and 7(b), the temperature was almost constant at the 1:00 p.m. of the first day, at which the concrete casting was almost completed. After 24 hours, the effect of hydration heat controlled and the temperature of the girder was higher than all compared days. As discussed in Fig. 6, it is clear in Fig. 7 that the effect of the top surface heating due to solar radiation was still less than the effect of hydration heat during the next day, in which the temperature of concrete cores was higher than the temperature of the top surface.

The temperature distribution at 1:00 p.m. of the second day is interesting. In aged concrete, the temperature of the top surface should be much higher than of other parts of concrete, but as shown in Fig. 7, the temperature of the top surface was lower than of interior parts of the webs. This result can be attributed to the amount of hydration heat that was released during the last 24 hours. The hydration heat raised the temperature of the interiors of the girder to such temperatures that still higher than the temperature gained at the surface due to solar radiation. In general, it can be noticed that the girder's average temperature decreased by about 7℃ compared to the last 12 hours. It should be mentioned here that the sky was partially cloudy during the first two days, thus the solar radiation reaching the surfaces was not maximum as shown in Fig. 3.

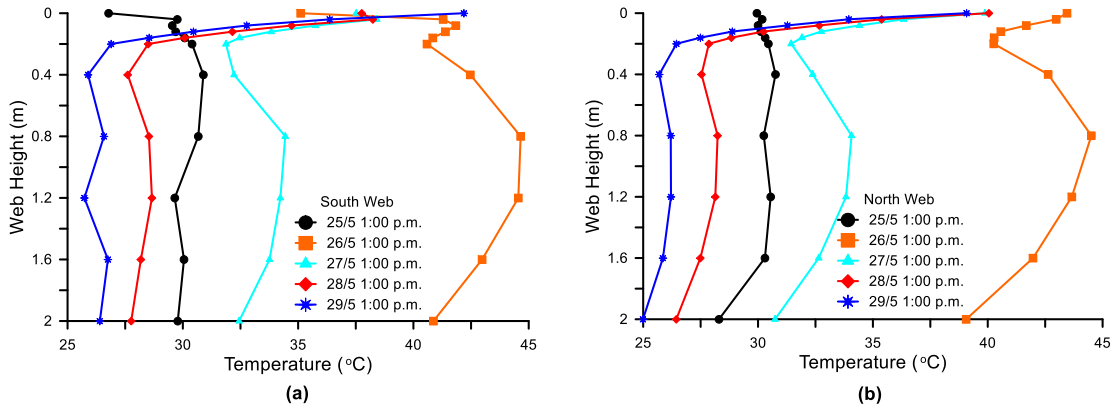

Figure 7 Vertical temperature distributions at 1:00 p.m. for the first five days (a) south web (b) north web

The effect of hydration heat decreased significantly after 48 hours from concrete pouring. As shown in Fig. 7, the vertical temperature distributions on 27, 28 and 29 May was approximately following the normal vertical distribution of aged concrete. Furthermore, the average temperature along the webs was decreasing with time after the first day. The temperature of the ambient air at 1:00 p.m. of the first four days was around 27℃, while for the fifth day it was 29.6℃. The average temperatures along the south web were about 43, 33, 28 and 26 ℃ at 1:00 p.m. of 26, 27, 28 and 29 May, respectively. This means that after about 100 hours, the effect of hydration heat became negligible.

Vertical Temperature Gradients

The vertical temperature gradients at 1:00 p.m. for the south web and the north web during the first five days are shown in Fig. 8, which were the calculated based on Fig. 7. As discussed in the previous section, the effect of hydration heat controlled the temperature distributions along the south web during the first 24 hours, thus as shown in Fig. 8(a), the gradients at 1:00 p.m. of 25 and 26 May were negative. On the other hand, the vertical temperature gradients along the south web and the north web at 1:00 p.m. of the following three days were positive with maximum at or near the top surface as shown in Figs. 8(a) and 8(b). The maximum vertical temperature gradient at the top surface increased with time due to the decreasing of the effect of hydration heat, which resulted in cooling down of the interior parts of the webs. The maximum temperature gradients at the top surface of the north web at 1:00 p.m. on 26, 27, 28 and 29 May were 4.4, 9.1, 13.6 and 14.1℃, respectively. On the other hand, the maximum positive temperature gradients at the top surface of the south web at 1:00 p.m. on 27, 28 and 29 May were 5.7, 10.2 and 16.5℃, respectively. The maximum vertical temperature gradient was recorded in the south web on 26 May at 2:00 a.m., which was 24.3℃.

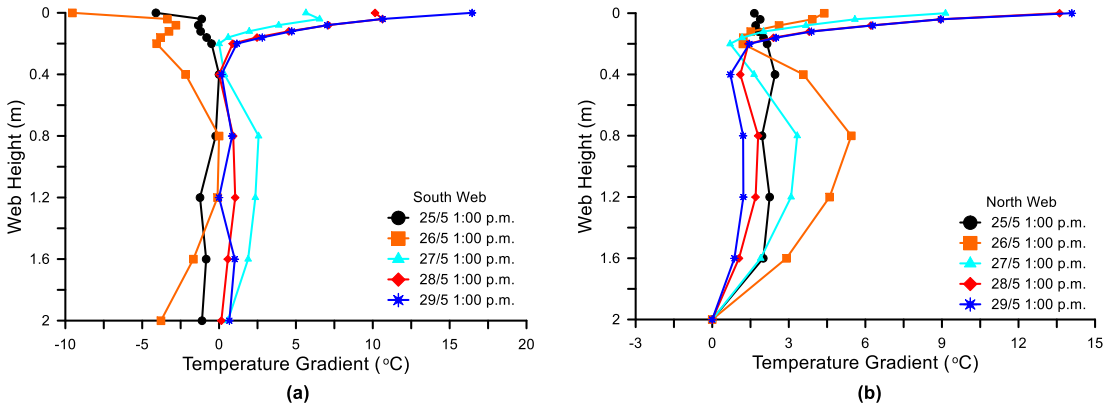

Figure 8 Vertical temperature gradients at 1:00 p.m. for the first five days (a) south web and (b) north web

Lateral Temperature Distributions

The distributions of temperature along the top slab at 1:00 p.m. for the first five days are shown in Fig. 9(a). Note that on May 25, the selected time is 1:30 p.m. instead of 1:00 p.m., this is because the concrete pouring of the top slab was not completed yet at 1:00 p.m.

Fig. 9(a) shows that temperature was almost the same along the top slab at 1:30 p.m. on 25 May. It is illustrated in Fig. 9(a) that the temperature of the top slab increased significantly after 24 hours because of the general increase in concrete temperature due to hydration heat. Moreover, the maximum temperatures were occurred near the top slab-south web junction. The thermocouples at the slab-web junction are surrounded with higher concrete mass than all other top slab's thermocouples, thus the heat of hydration results in higher temperature than other parts. The orientation of the longitudinal axis of the bridge (East-West) and the season (end of spring) led to higher heating of the south web during the day hours than the north web.
As concluded in the previous sections, the effect of hydration heat decreased significantly after 48 hours and almost diminished after approximately 100 hours, this result is also obvious in Fig. 9(a). The temperature distributions along the top slab became more stable after 48 hours, where the temperature distributions of the 27, 28 and 29 of May were almost the same. The only distinguishable difference is the average temperature of thermocouples, which decreased with time as shown in Fig. 9(a).
Fig. 9(b) shows the temperature distribution along the top slab during the early morning hours of the subsequent five days. It is clearly shown that the effect of heat hydration reached its peak in the night following the pouring day (on 26 May at 4:00 a.m.). The following two nights showed lower effect of hydration heat than the first night, but the effect was still significant.
Air temperatures during the same time steps illustrated in Fig. 9(b) were 11.3, 17.6, 17.2, 13.0 and 11.0 ℃ on 26, 27, 28, 29 and 30 May, respectively. While the maximum temperature of concrete at the top slab at the same time steps were 35.8, 31.4, 28.8, 24 and 23.9℃, respectively. This means that as time passes, the concrete temperature tended to be close to air temperature.

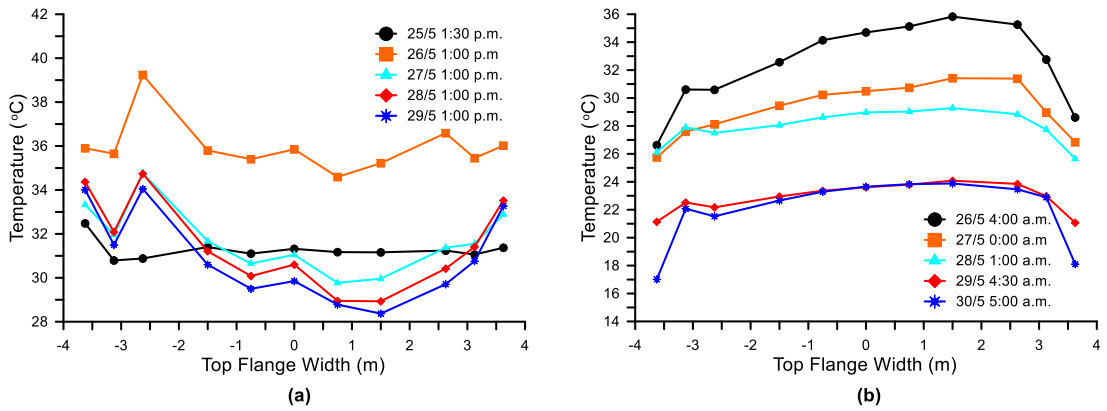

Figure 9 Temperature distributions along the top slab for the first five days (a) afternoon (b) morning

Fig. 10 shows the temperature distributions along the bottom slab at 1:00 p.m. during the first five days. The behavior of temperature along the bottom slab was in general the same, where the maximum temperatures occurred at the outer ends of the slab, while temperature was almost uniform along the rest length of the bottom slab. This behavior was obviously different from that of the top slab. This difference was mainly due to the location of each slab and its geometrical configuration. The top slab was almost completely exposed to solar radiation along the whole day hours, while the bottom slab was partially shaded. The cantilever ends of the top slab had

also their effect on the shading of the side ends of the bottom slab during the mid day. The higher speed of air at the top surface led to faster cooling than the bottom surface during the night.

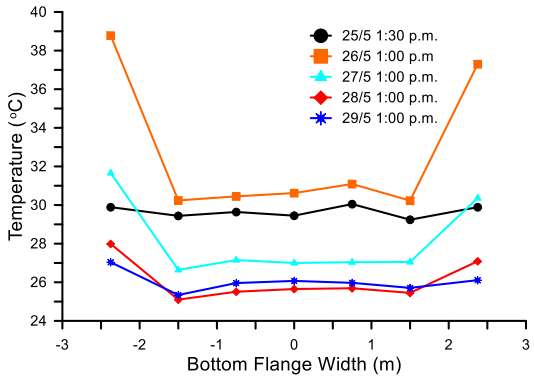

Figure 10 Afternoon temperature distributions along the bottom slab for the first five days

Conclusions

From the results of the thermocouples and the environmental sensors of the full-scale experimental concrete box-girder segment that carried out in this study, the following conclusions can be drawn,

1- During the early age of concrete, the effect of hydration heat was significant, both on the individual temperature-time curves of thermocouples and on the temperature distributions and gradients along the webs and the slabs of the box-girder.

2- The effect of hydration heat reached its maximum after about 12 hours, at which the recorded maximum vertical temperature gradient was approximately 25℃. After 48 hours, the effect of hydration heat decreased significantly, while it diminished after about 100 hours.

3- The effect of hydration heat on temperature readings influenced mainly by the location of thermocouples, the distance from the nearest exposed surface and the degree of sealant from formwork. Interior thermocouples that were surrounded by larger mass of concrete and those that were completely sealed by formwork were most influenced by thermal heat. S7 and N7 thermocouples that were located below the top slab-web junctions showed the higher temperatures and followed the behavior of hydration heat with time. On the other hand, the surface thermocouples S1 and N1 showed much lower dependency on hydration heat, their temperatures during the peak of hydration heat (about 10 to 12 hours after concrete pouring) were the lowest among all thermocouples. Surface thermocouples followed the fluctuation of air temperature with time even during the early hours of concrete age.

4- Due to the effect of hydration heat, the temperatures of the webs' interior thermocouples kept higher than of the surface thermocouples during most of day hours of the next day, thus caused negative vertical thermal gradients in spite of the gradual worming of the top surface by solar radiation. After 48 hours, this effect decreased significantly and the vertical temperature gradients became closer to those of aged concrete with positive gradients during the day hours and negative gradients during the night hours.

5- The effect of hydration heat on the lateral temperature distributions along the top and the bottom slabs was clear during the first days, during which the average temperatures of the slabs increased noticeably, although, the temperature gradients of top slab showed higher dependency

on air temperature during the day hours. The configuration and the boundaries of the bottom slab, kept a degree of independency for the behavior of temperature gradient of the bottom slab during the day hours of all days, during which the effect of shading from webs was significant.

References

1. White IG. *Nonlinear Temperature Differential Distributions in Concrete Bridge Structures: A Review of The Current Literature*. Technical Report 525, Cement and Concrete Association: USA, 1979.
2. Imbsen RA, Vandershaf DE, Schamber RA, Nutt RV. *Thermal Effects in Concrete Bridge Superstructures*. National Cooperative Highway Research Program Report 276, Transportation Research Board: Washington, DC, USA, 1985.
3. Elbadry M, Ghali A. Thermal stresses and cracking of concrete bridges. *ACI Journal* 1986; **83**(6): 1001-1009.
4. Massicotte B, Picard A, Gaumond Y, Ouellet C. Strengthening of long span prestressed segmental box girder bridge. *PCI Journal* 1994; **39**(3): 52-65.
5. Li D, Maes MA, Dilger WH. Thermal design criteria for deep prestressed concrete girders based on data from confederation bridge. *Canadian Journal of Civil Engineering* 2004; **31**(5): 813-825.
6. Pisani MA. Non-linear strain distributions due to temperature effects in compact cross-sections. *Engineering Structures* 2004; **26**(10): 1349-1363.
7. William GW, Shoukry SN, Raid MY. Early age cracking of reinforced concrete bridge decks. *Bridge Structures* 2005; **1**(4): 379-396.
8. Chen B, Ding R, Zheng J, Zhang S. Field test on temperature field and thermal stress for prestressed concrete box-girder bridge. *Frontier of Architecture and Civil Engineering in China* 2009; **3**(2): 158-164.
9. Bentz DP, Stutzman PE, Sakulich AR, Weiss WJ. *Study of Early-Age Bridge Deck Cracking in Nevada and Wyoming*. NISTIR Report 7841, National Institute of Standards and Technology: USA, 2012.
10. Neville AM. *Properties of Concrete*. Pearson Education Limited: Edinburgh, UK, 2011.
11. Ghali A, Favre R, Elbadry M. *Concrete Structures: Stresses and Deformation*. Spon Press: London, UK, 2002.
12. BS 5400-2:1978. *Steel, Concrete and Composite Bridges: Specifications for Loads*. British Standards Institution: London, UK, 1999.
13. AASHTO. *AASHTO LRFD Bridge Design Specifications*. American Association of State Highway and Transportation Officials: Washington DC, USA, 2012.
14. AS 5100.2-2004. *Bridge Design: Part2: Design Loads*. Standards Australia: Sydney, Australia, 2004.